



# Effect of Alternative Fuels on Soot Properties and Regeneration of Diesel Particulate Filters

**Juhun Song, Mahabubul Alam and André Boehman**

**Department of Energy and Geo-Environmental Engineering**

**The Penn State Energy Institute**

**College of Earth and Mineral Sciences**

**The Pennsylvania State University**

**Sponsors:**

**ConocoPhillips**

**National Energy Technology Laboratory**

**Pennsylvania Department of Environmental Protection**

**Cummins Engine Company**



# Background

- **Observations of a soot nanostructure-oxidative reactivity relationship, reported at DEER 2004, evidenced by lower regeneration temperature for biodiesel (B20) blends and greater oxidation rates in TGA/DSC measurements as well as in on-engine DPF regeneration tests – what is the source of this difference in PM regeneration process and how do these soots behave during oxidation ?**
- **Vander Wal et al. published in *Combustion & Flame* in 2003 and 2004 papers demonstrating: (1) differences in the structure within soot primary particles with benzene, ethanol and acetylene, and (2) particles with less ordered structure provided higher oxidative reactivity**



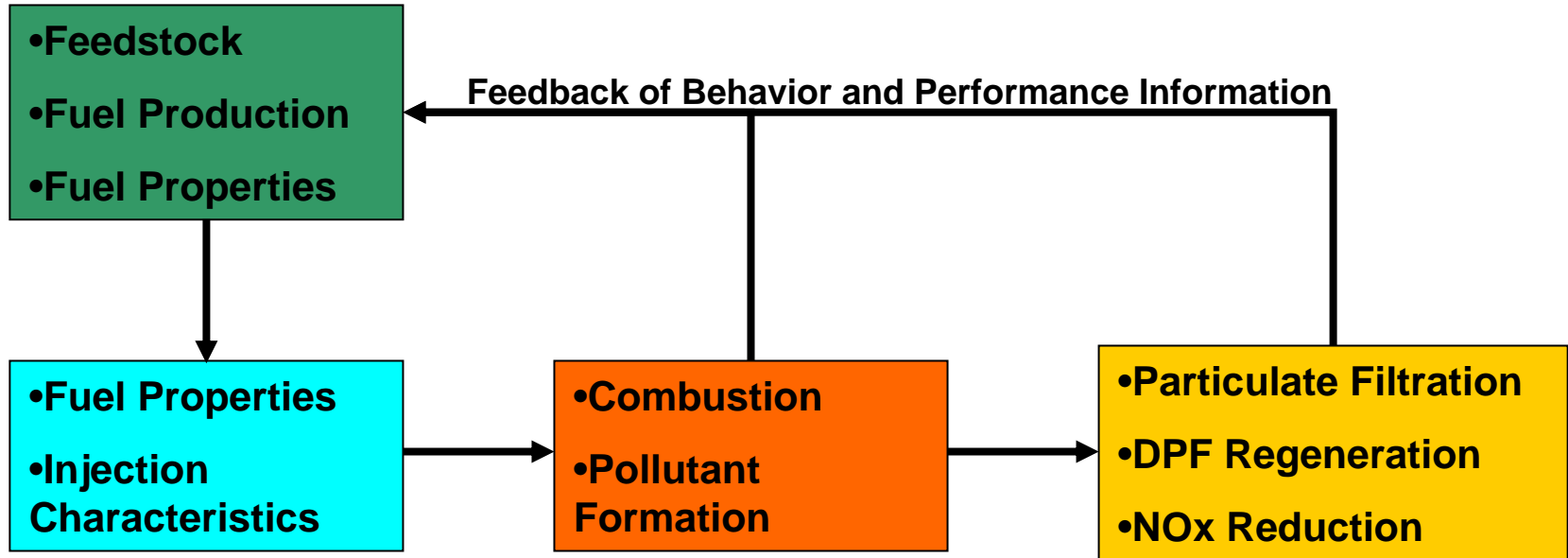
# Objectives

## Ultra Clean Fuels Project

- **Determine the Interaction between Formulation of Conventional, Renewable and Synthetic Diesel Fuels and their Injection Characteristics**
- **Measure Physical Properties of Fuels that Can Provide Support for Understanding Injection, Combustion and Emissions Performance of Diesel Fuels**
- **Use Injection Studies, Physical Properties, Emissions Measurements and In-Cylinder Visualization to Determine Optimal Fuel Formulations**
- **Link Feedstock and Fuel Production Process to Physical Properties and, Thereby, Injection, Combustion and Emissions Performance - *Characteristics of Soot from Different Fuels – Considering Neat Alternative Fuels, B100 and FT100***



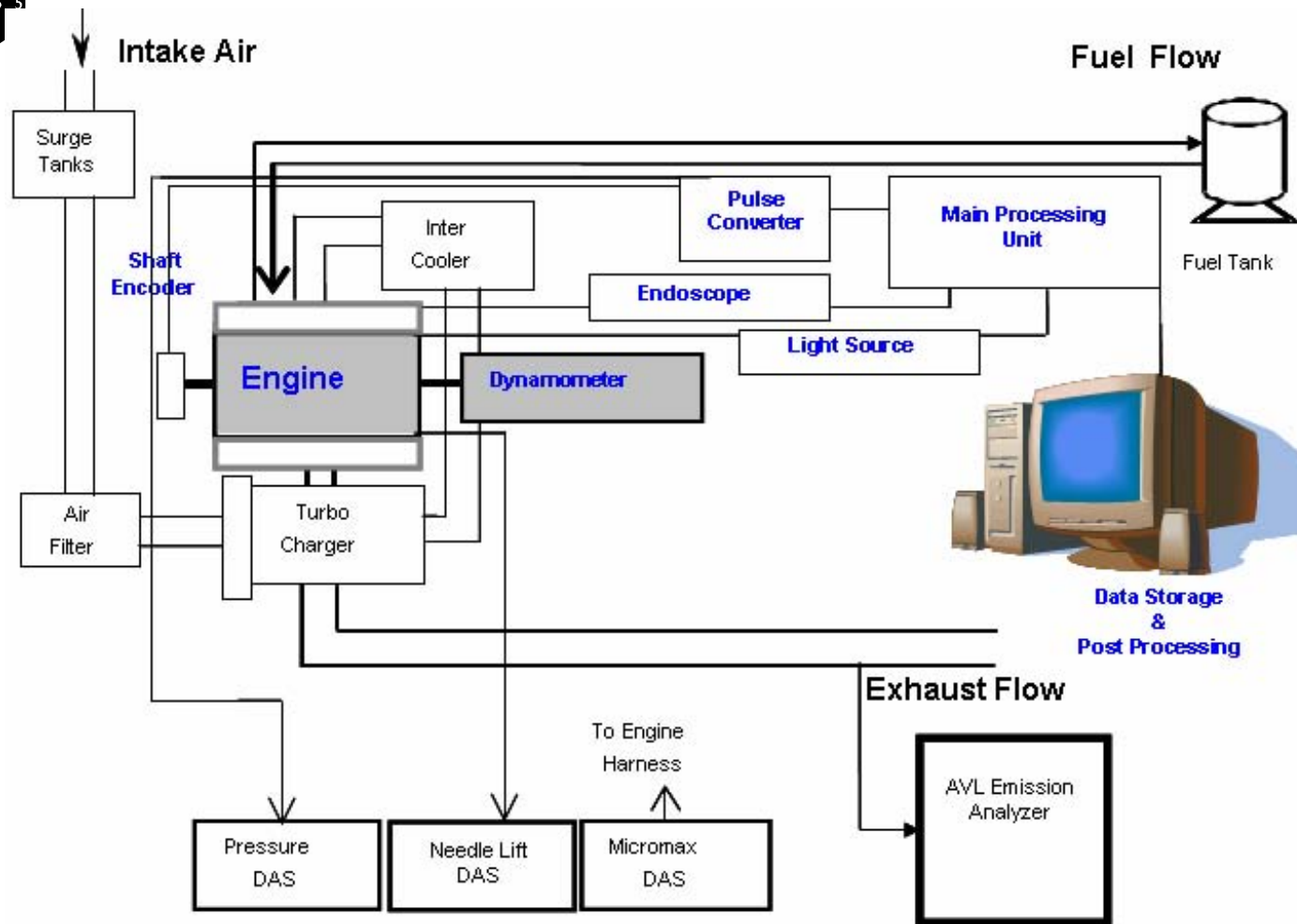
# Research Strategy



- Spray Visualization Chamber
- Bulk Modulus of Compressibility

- AVL 513D Engine Videoscope
- Particulate and Gaseous Emissions

- Various Aftertreatment Strategies



**Schematic diagram of the Cummins ISB test stand**



# Outline

## Ultra Clean Transportation Fuels from Natural Gas

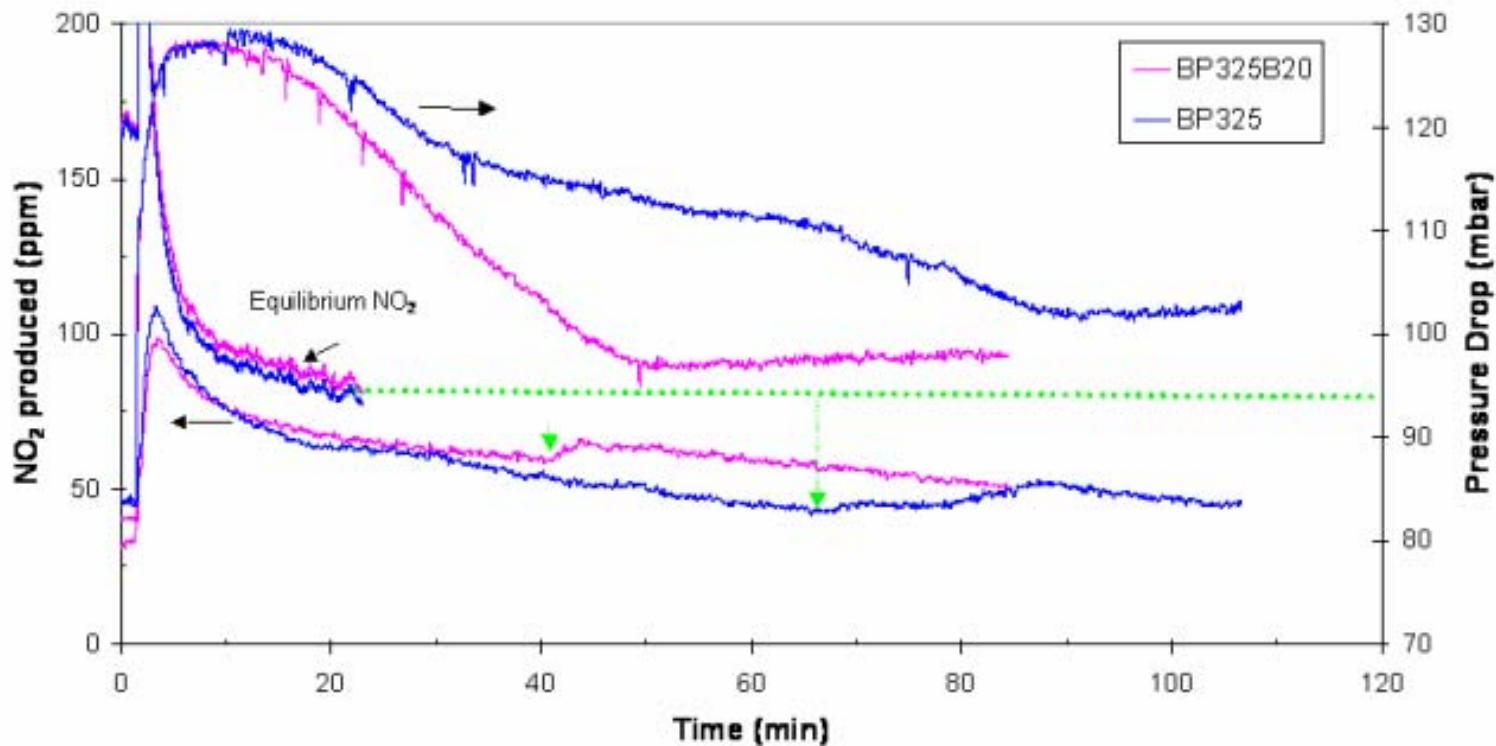
- **Review of Key Observations Reported at DEER 2004**
- **Influence of Fuels, Injection Timing, Combustion and Emissions on the Performance of Aftertreatment Devices**  
→ *Characteristics of Soot from Different Alternative Fuels*



# Fuel Composition Effects on Emissions

BP-325 and BP-325/B20 Test Fuels in a High Temp Regeneration

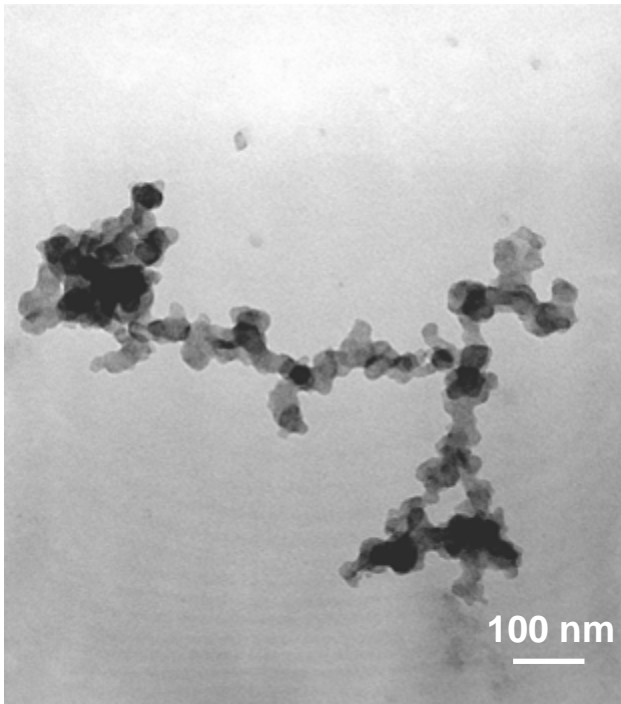
Regeneration Rate's Dependence on NO<sub>2</sub> produced



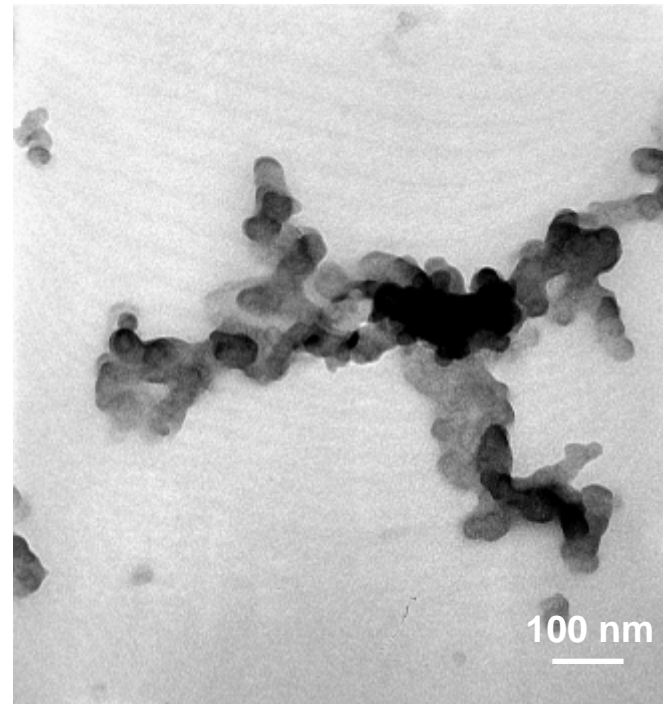


# Variation in Heavy Hydrocarbon Fraction

## Soot Morphology



(c) BP15 Derived PM

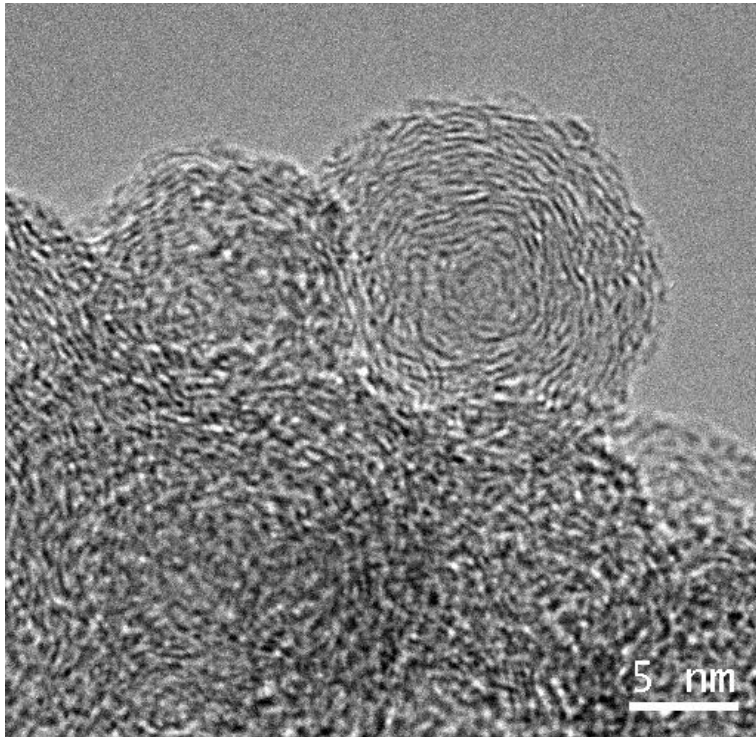


(d) BP15B20 Derived PM

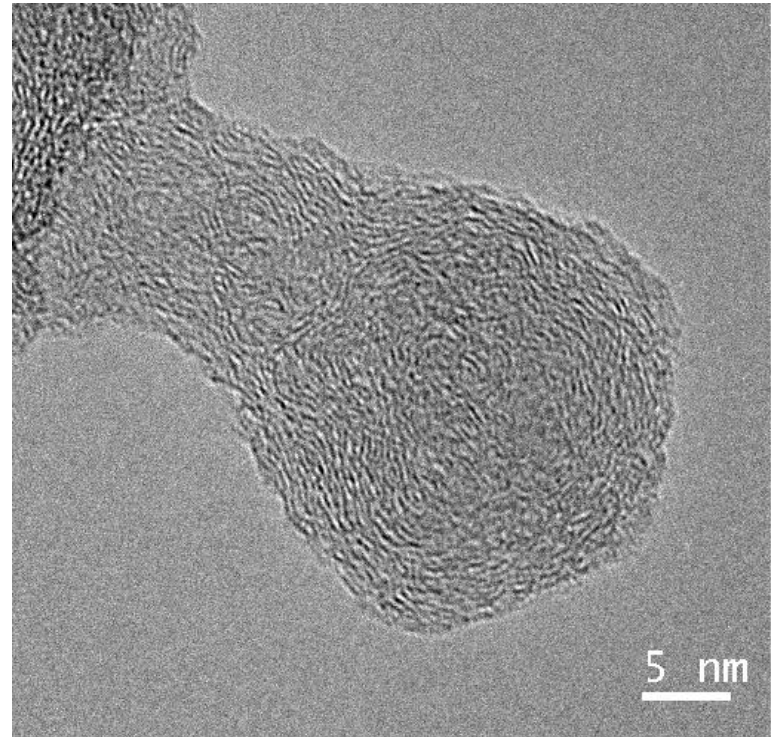


## *Initial Results – Comparing Diesel and B20*

### **Soot Nanostructure – Less Ordered Nanostructure Corresponds to Enhanced Reactivity**



**(a) BP15 Derived PM**

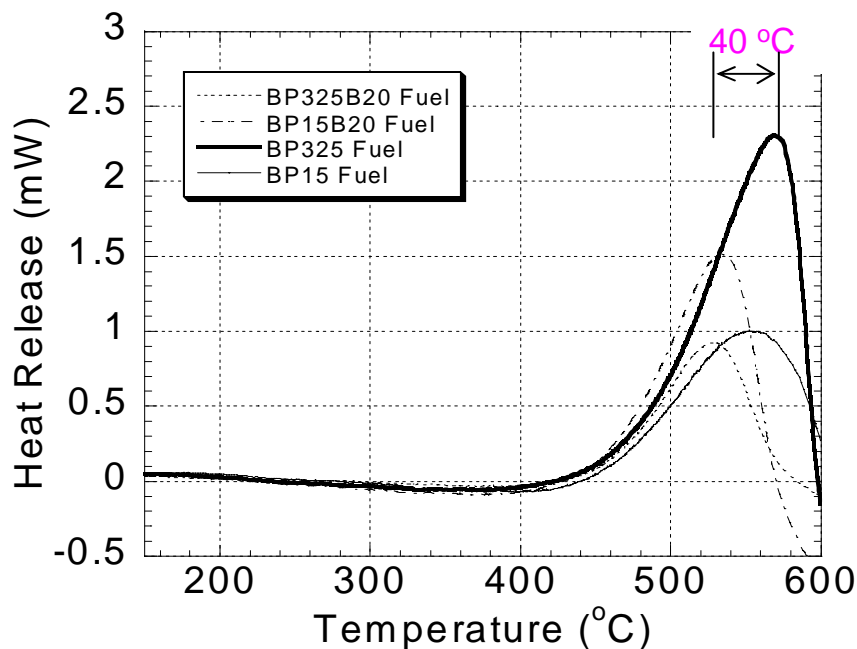


**(b) BP15B20 Derived PM**

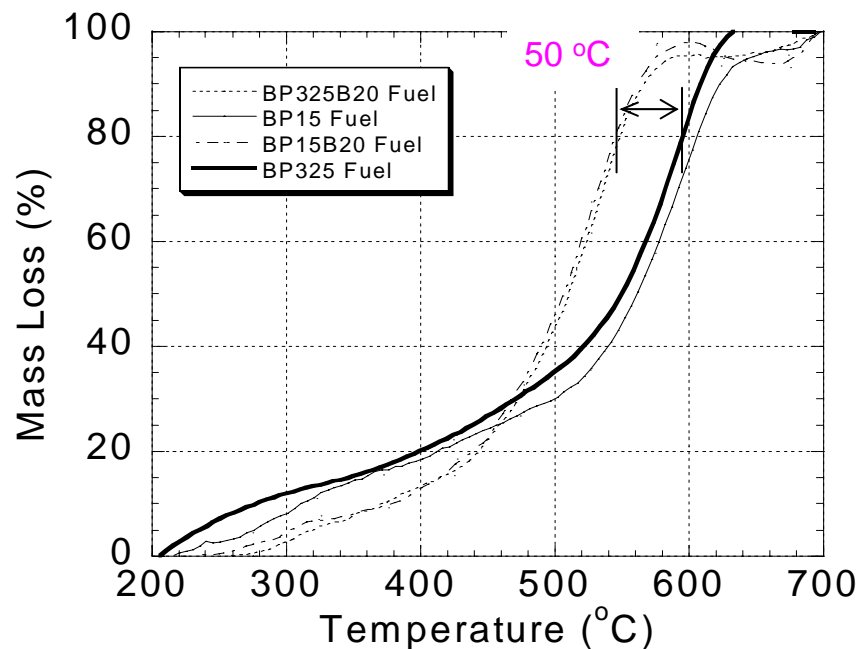


# Soot Nanostructure and Its Effect on Reactivity

**Low temperature Reactivity from DSC/TGA test**  
 - under 21% oxygen gas with treated samples



(a) Burning rate DSC curve

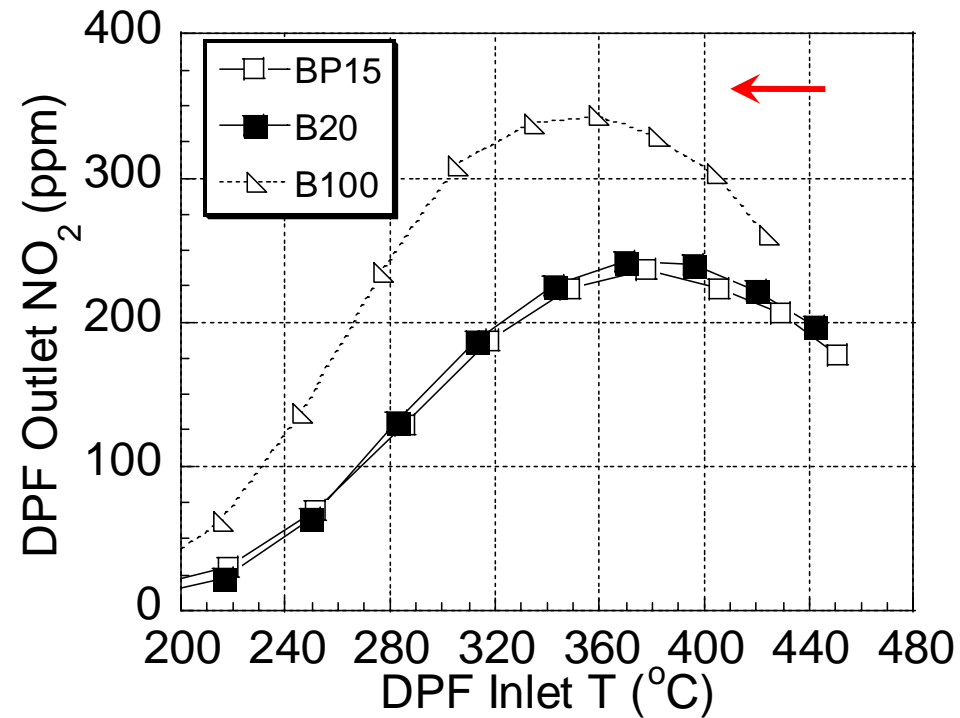
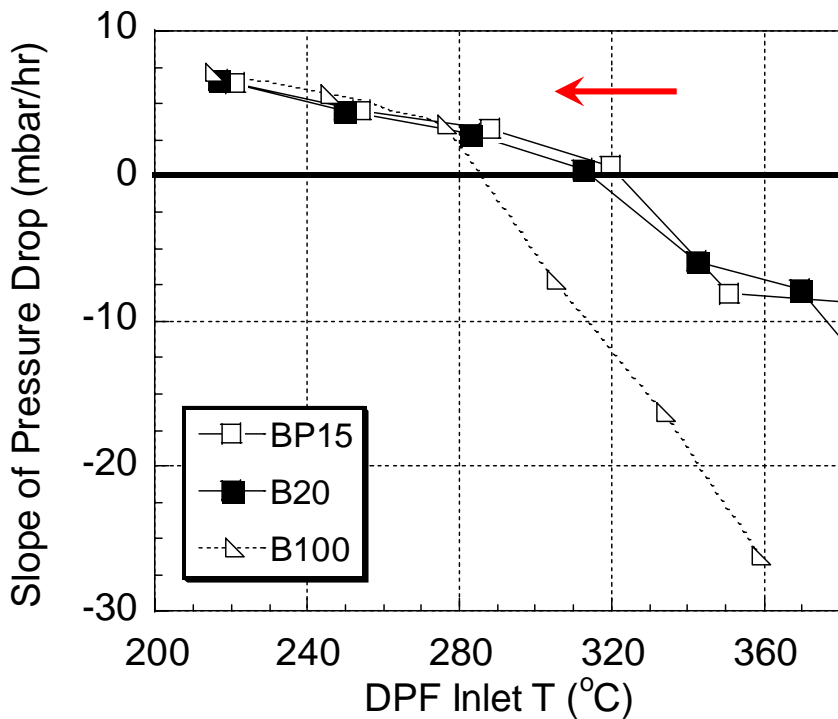


(b) Mass reduction TGA curve



# Expanded Results – Comparing Diesel, F-T and B100

## Low Temperature Regeneration

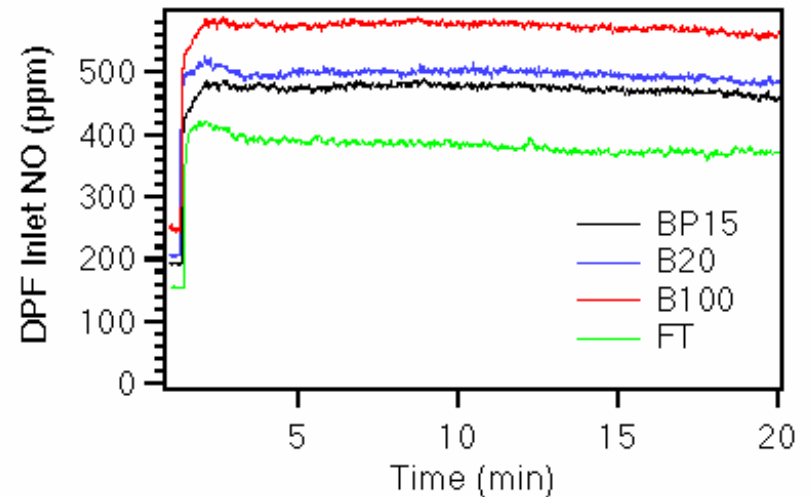
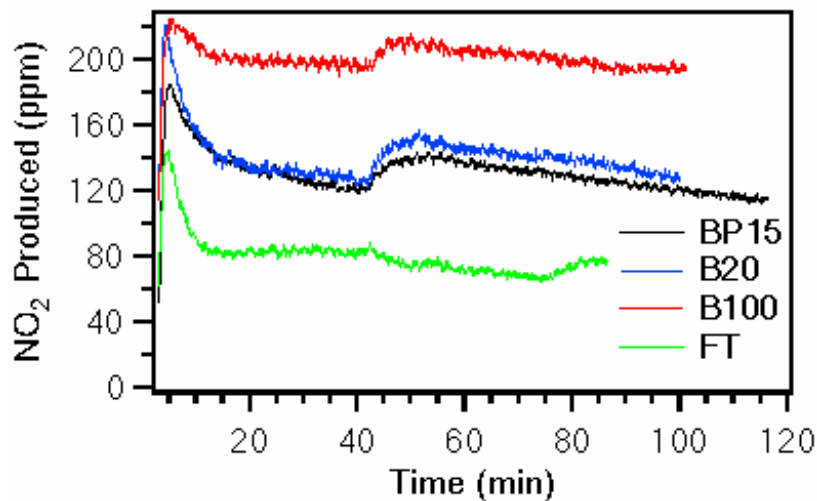
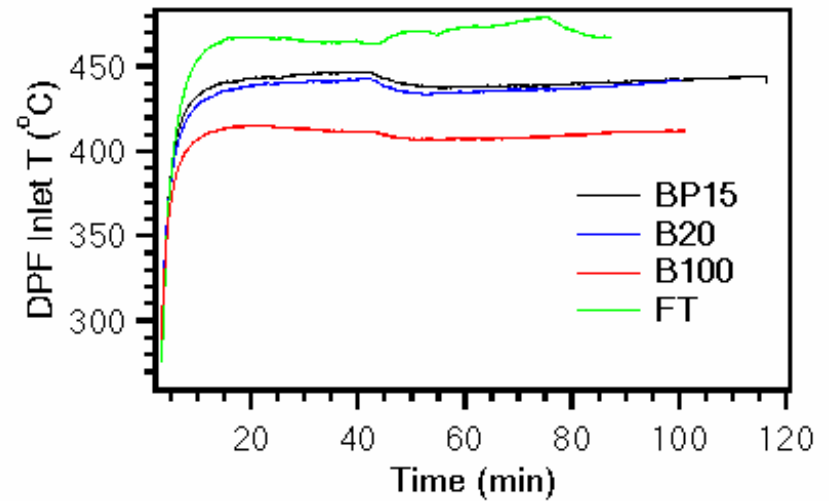
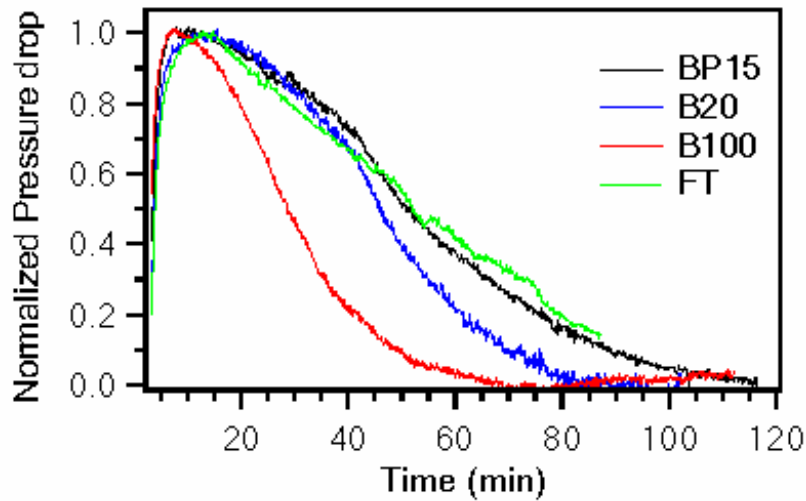


BET Temperature to be lower by **30 °C** with B100

**30 °C** shift of temperature where maximum NO<sub>2</sub> is produced over DPF

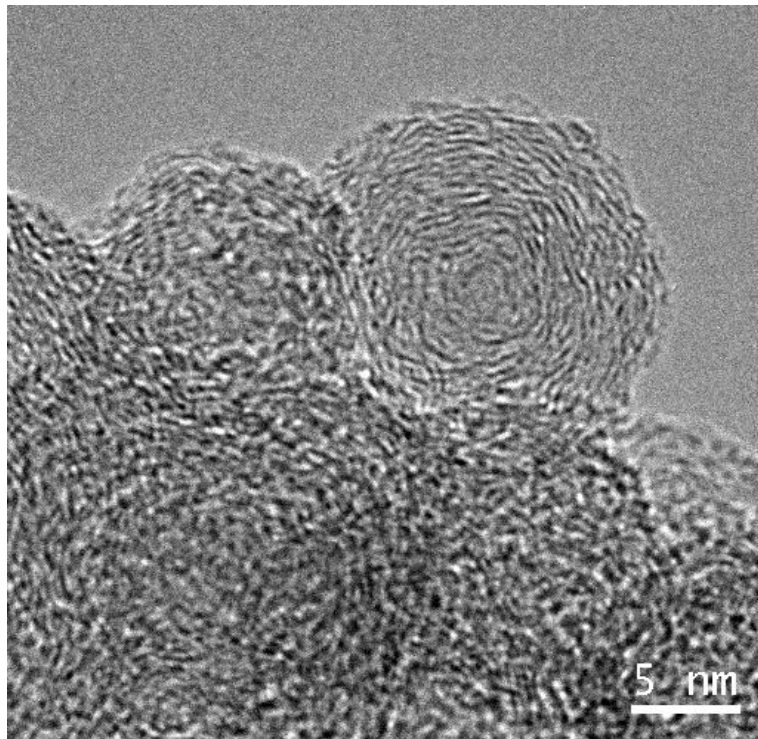


# High Temperature Regeneration (from 280 to 450 °C)

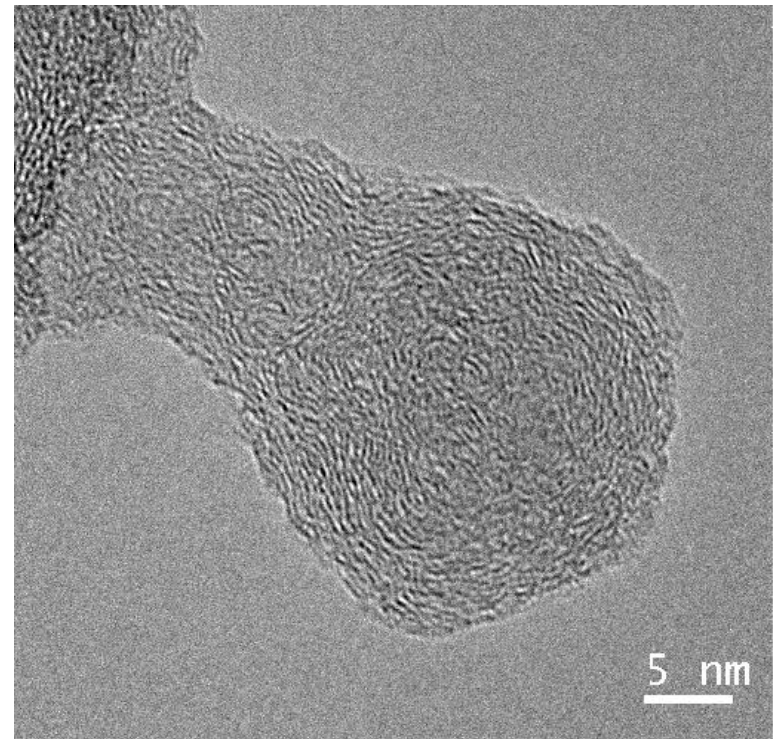




## Electron Microscopy of Initial Soot Nanostructure



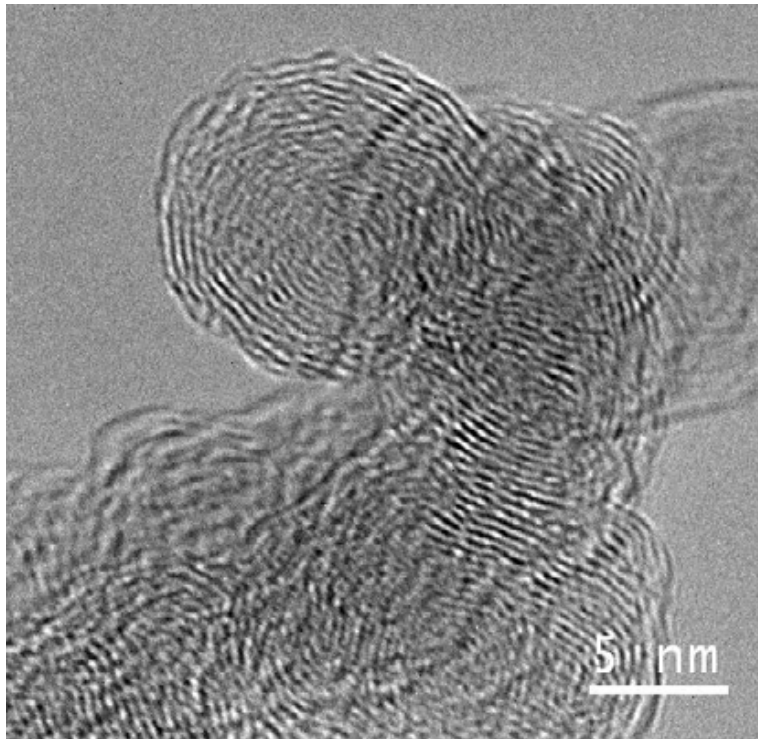
(a) BP15 Derived PM



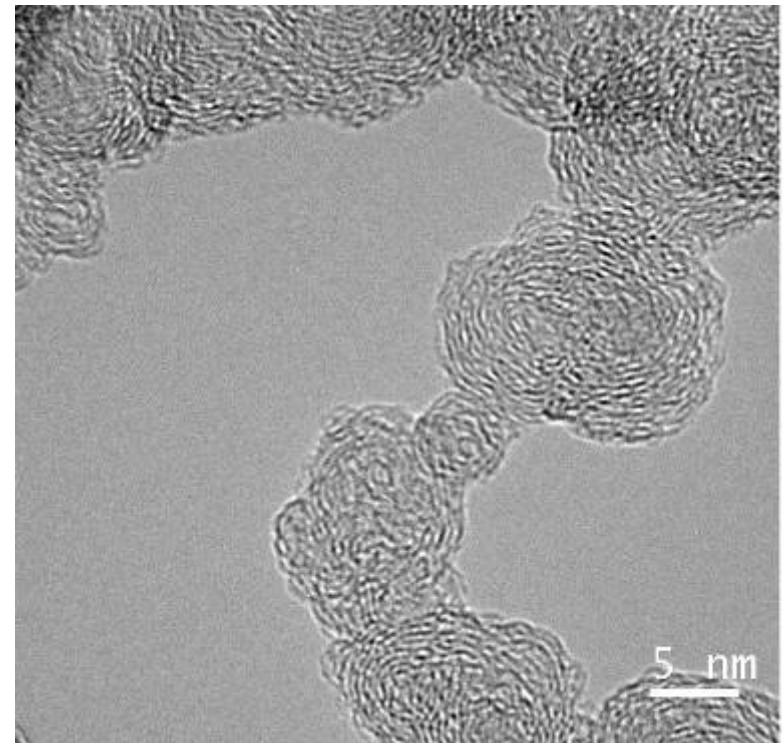
(b) BP15B20 Derived PM



## Initial Soot Nanostructure



**(c) B100 Derived PM**



**(d) F-T diesel Derived PM**

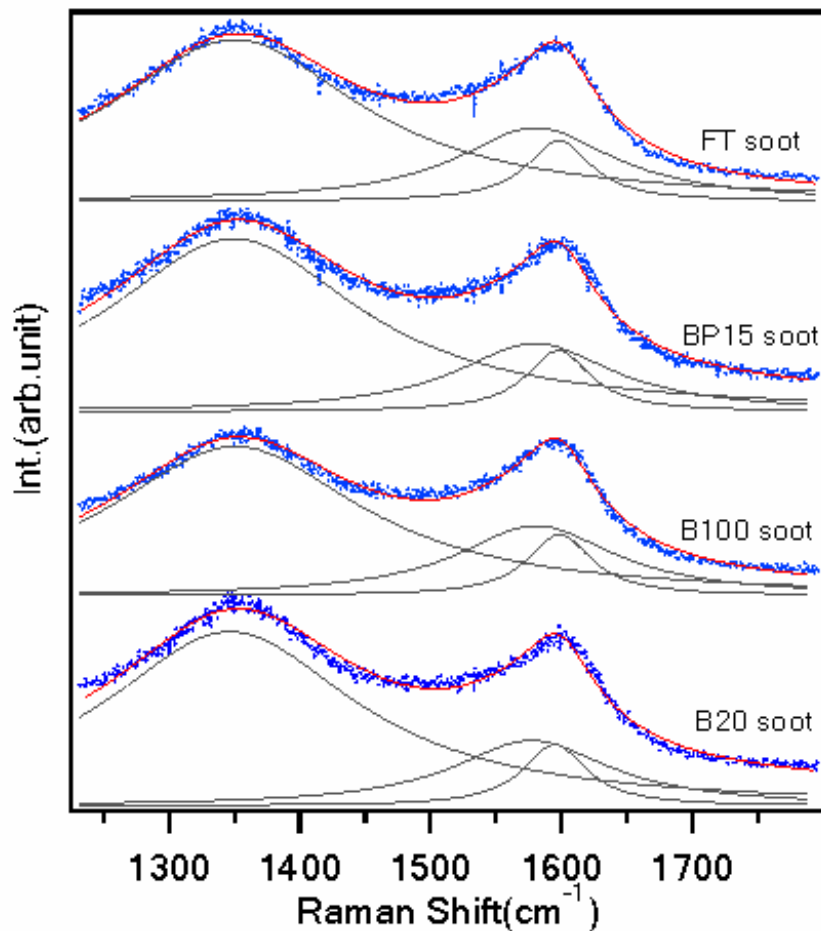


# Summary

- **From a comparison of DPF regeneration behavior**
  - ➔ **Enhanced regeneration of B100 in terms of both rate and BET is observed, whether this comes from particulate reactivity or catalyst activity which is sensitive to fuel sulfur**
  - ➔ **This difference in oxidation rate of DPF soot cake is reproduced in mass based rate on TGA as will be shown**



# Raman Analysis of Initial Structure



$I_d/I_g$  was extracted from 2 curves deconvoluted after lorentzian curve fitting

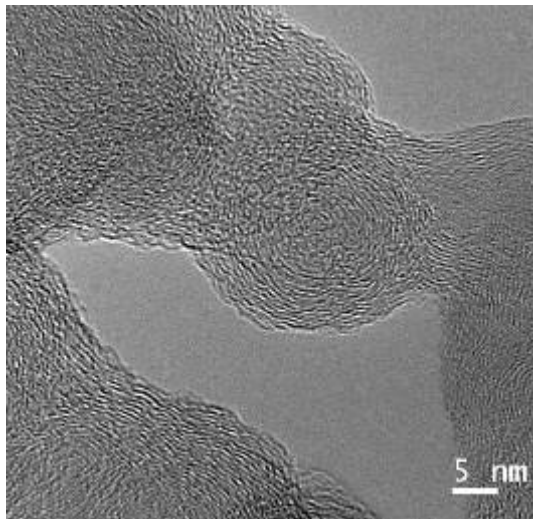
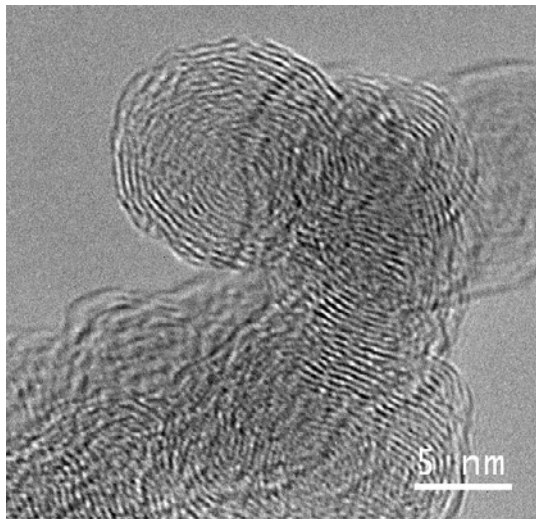
| Gra-<br>phitic<br>order | Soot type | D<br>band<br>cm <sup>-1</sup> | G band<br>cm <sup>-1</sup> | $I_d/I_g^*$ |
|-------------------------|-----------|-------------------------------|----------------------------|-------------|
| 3                       | BP15      | 1354                          | 1598                       | 1.11        |
| 4                       | B20       | 1354                          | 1598                       | 1.18        |
| 1                       | B100      | 1354                          | 1598                       | 1.06        |
| 2                       | FT        | 1354                          | 1598                       | 1.12        |
|                         | Graphite  | 1354                          | 1583                       | 0.37        |

Error bar : ±5% (± 0.05)

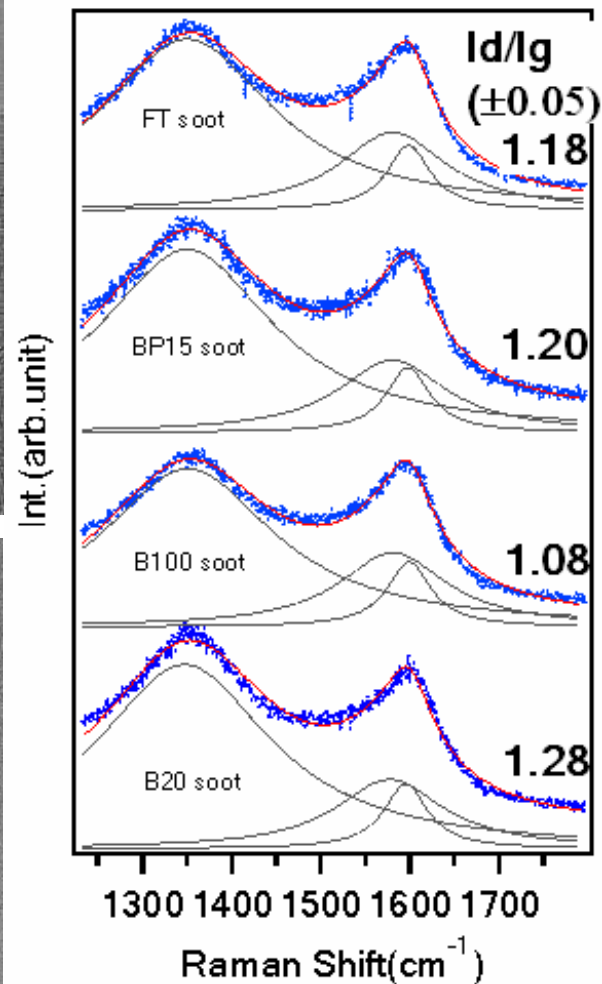
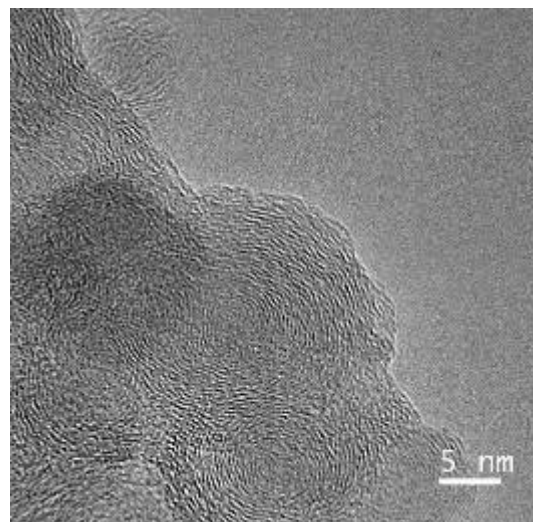
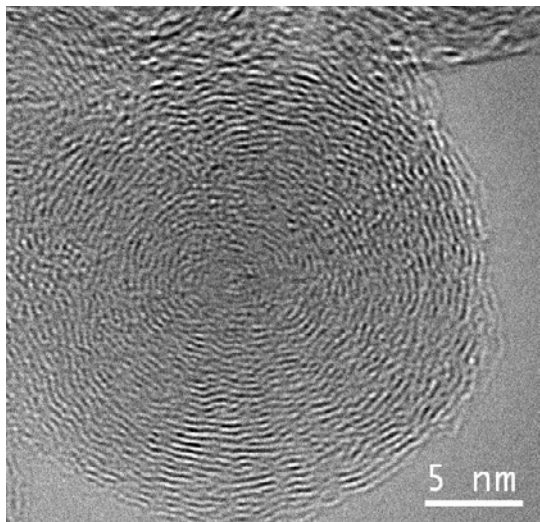


# Raman Analysis of Initial Structure

(a) B100



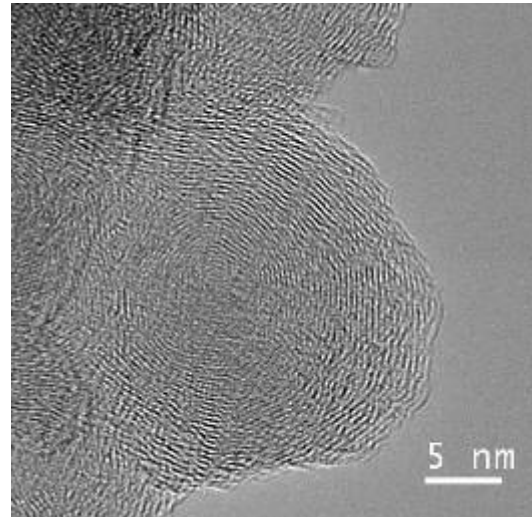
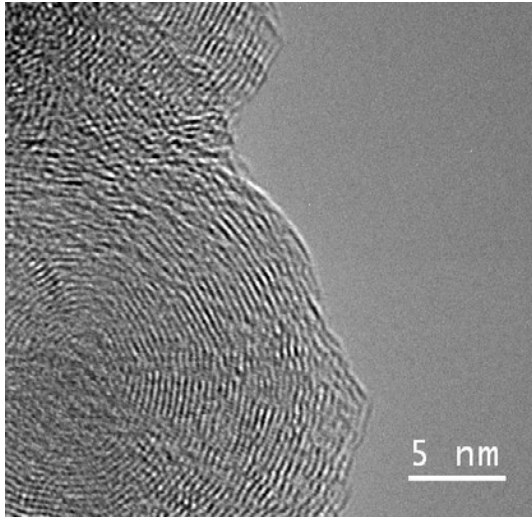
(b) FT



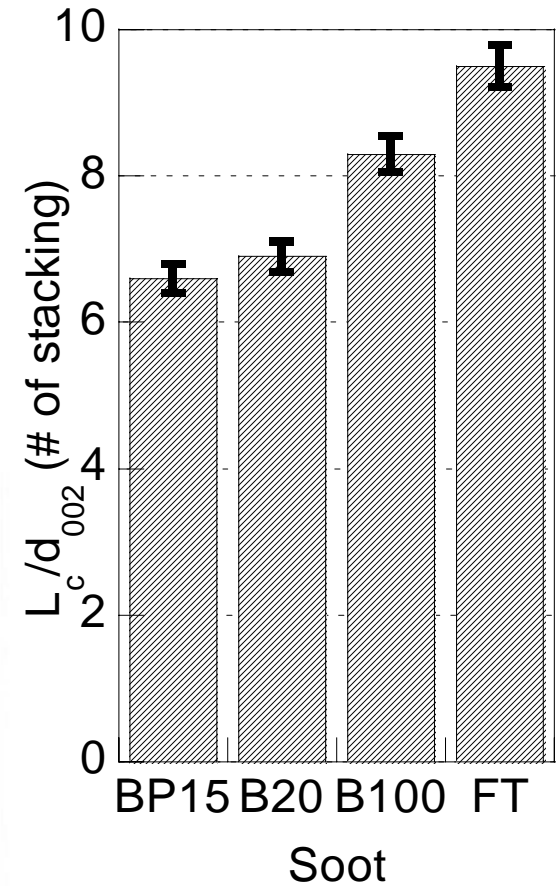
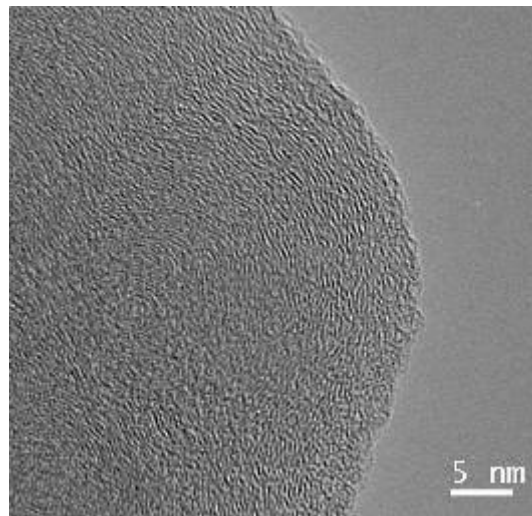
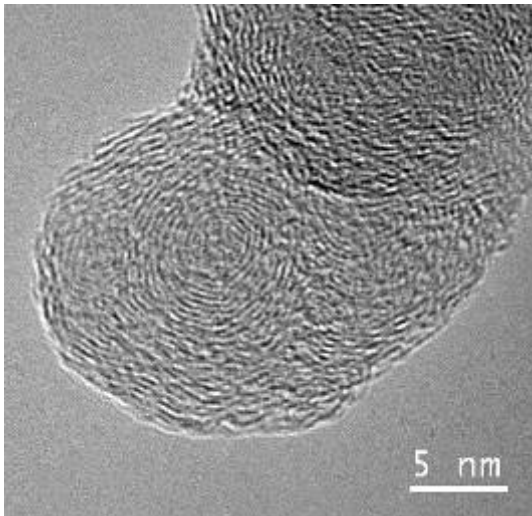


# XRD Analysis of Initial Structure

(c) BP15



(d) B20



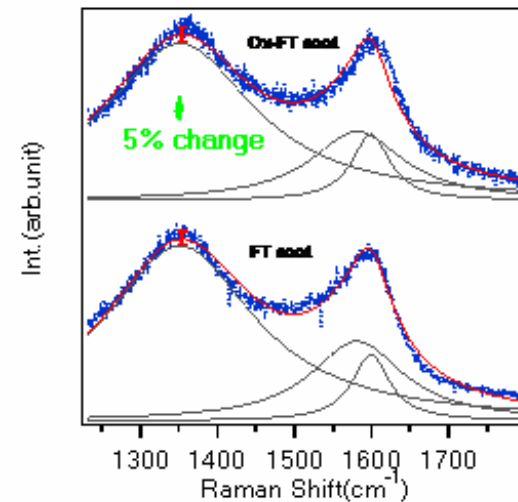
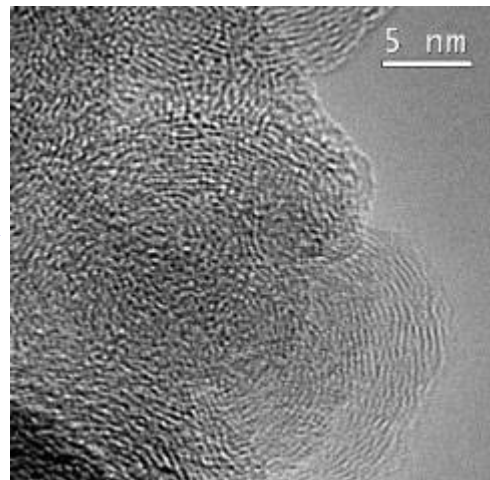
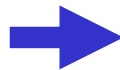
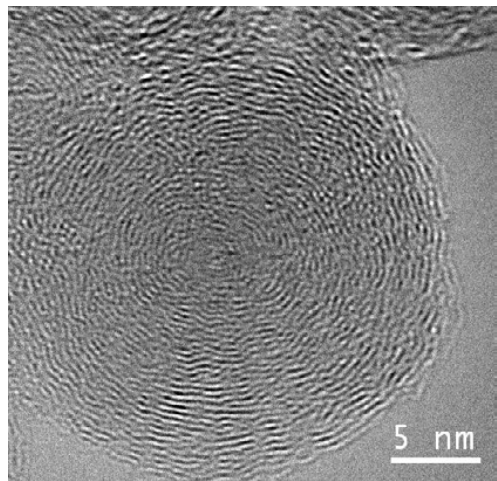


# Structural Change During Early Stage of Oxidation (30min)

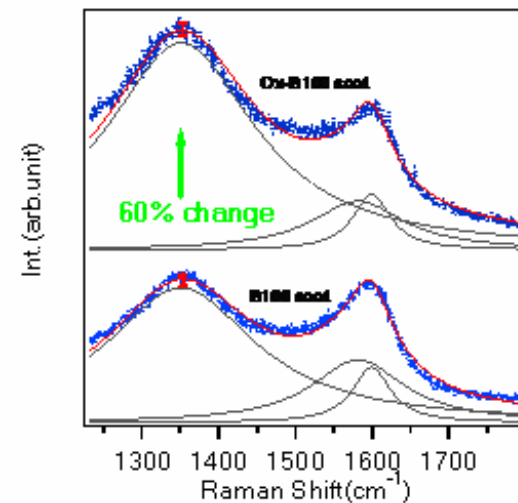
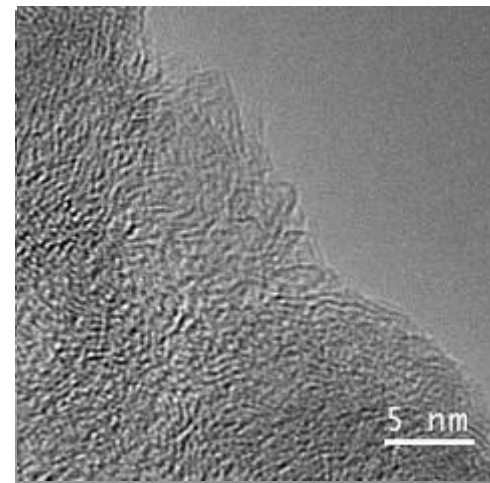
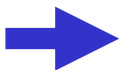
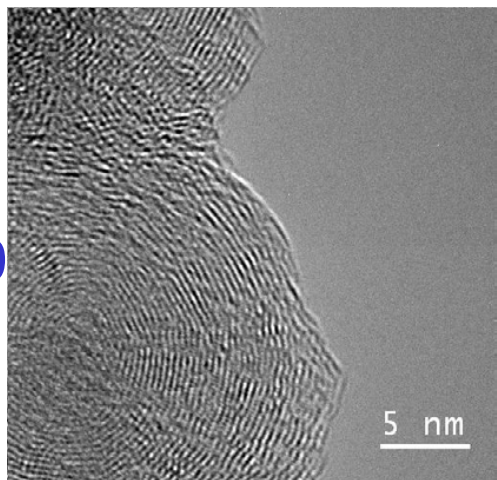
Initial

Oxidized

FT

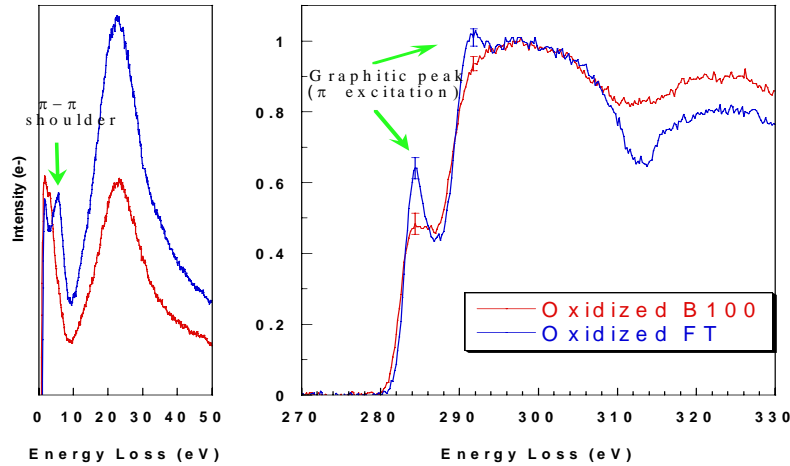


B100





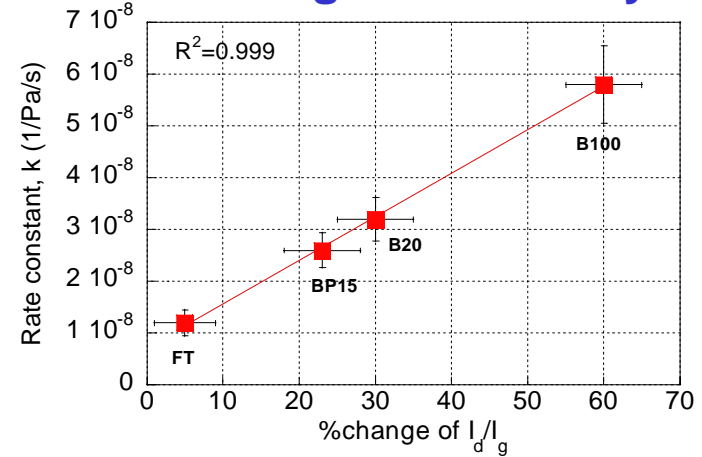
### Electron Energy Loss Spectra



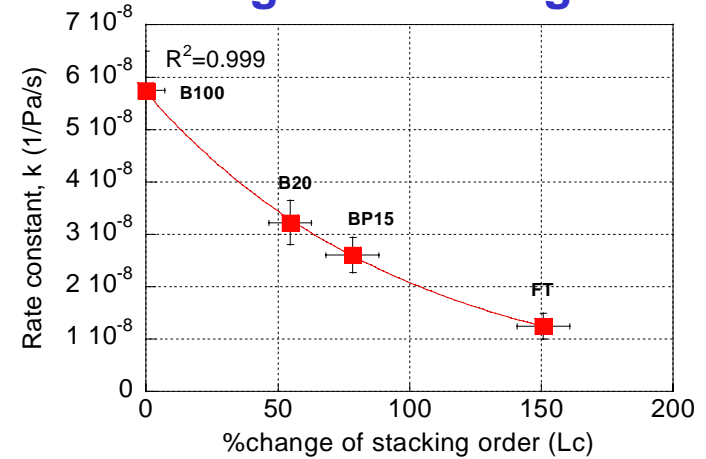
### % change of $I_{\pi}/I_{\sigma}$ ratio by EELS

| Soots | Before | After                   | %Change |
|-------|--------|-------------------------|---------|
| FT    | 0.642  | 0.610<br>( $\pm 0.03$ ) | -2      |
| B100  | 0.650  | 0.489<br>( $\pm 0.03$ ) | -26     |

### % change to defect by Raman



### % change of stacking order by XRD

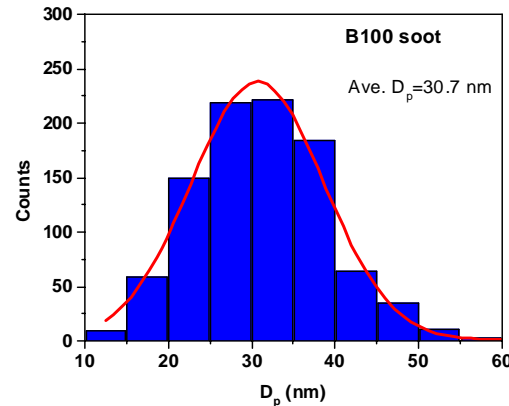
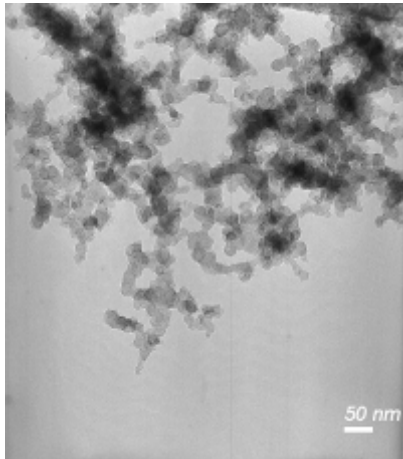


# Surface Area Based Oxidation Rate

## Comparison of surface area and mass based oxidation rate

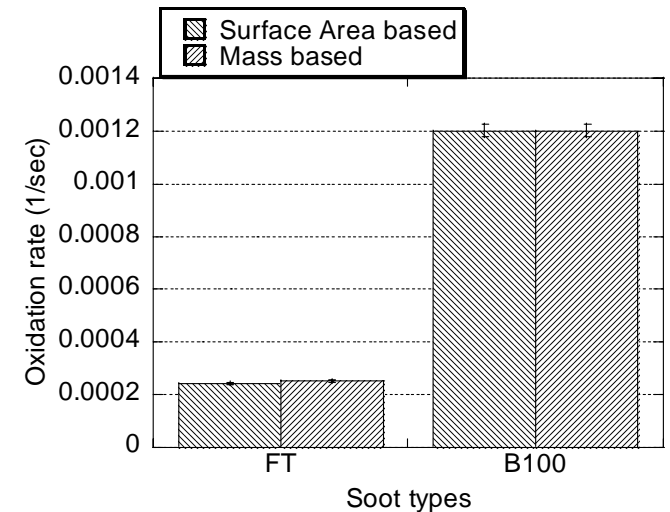
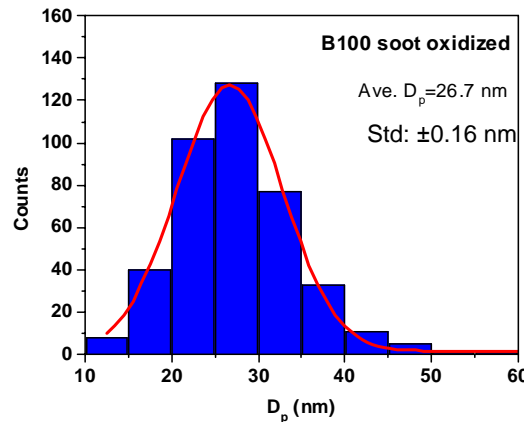
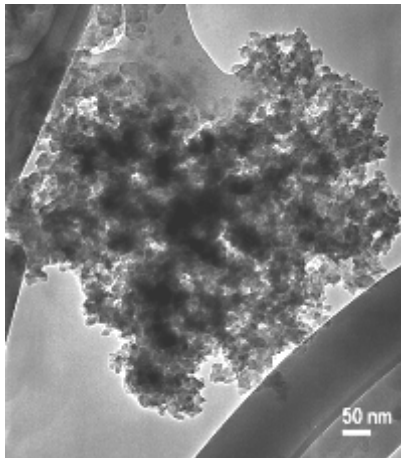
**B100**

**Initial**



← -4.0 nm

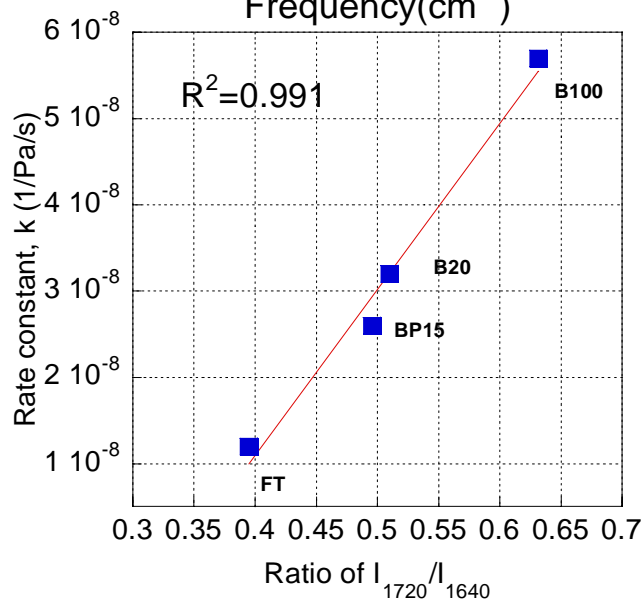
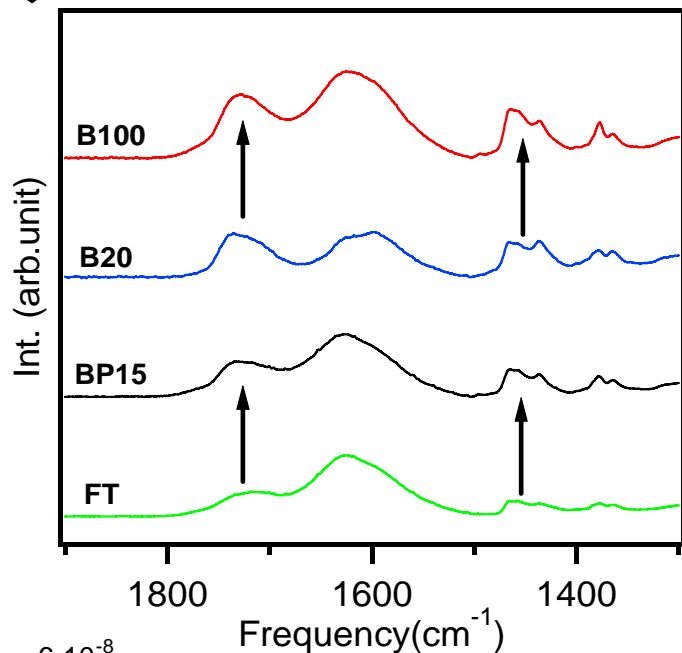
**Oxidized**



**Remaining Question : Under surface burning, why did B100 soot undergo severe structural change even though its initial nanostructure was the same as for FT soot ?**



# Oxygen Functionality of Initial Soot Samples



## IR spectra band assignment

| Range (cm <sup>-1</sup> )        | Chemical group                                       |
|----------------------------------|--|
| 1700                             | Lactone, Carboxyl<br>(bonded to two O or OH atoms)   |
| 1600<br><i>Under controversy</i> | Aromatic C=C stretch<br>C=O conjugated with aromatic |
| 1450                             | Aliphatic C-H  |
| 1400                             | Sulfate  |
| 1250                             | Ether, Phenol  |
| Below 1200                       | Electronic Noise due to high absorption of Kbr       |

From Fanning, Boehm, Smith



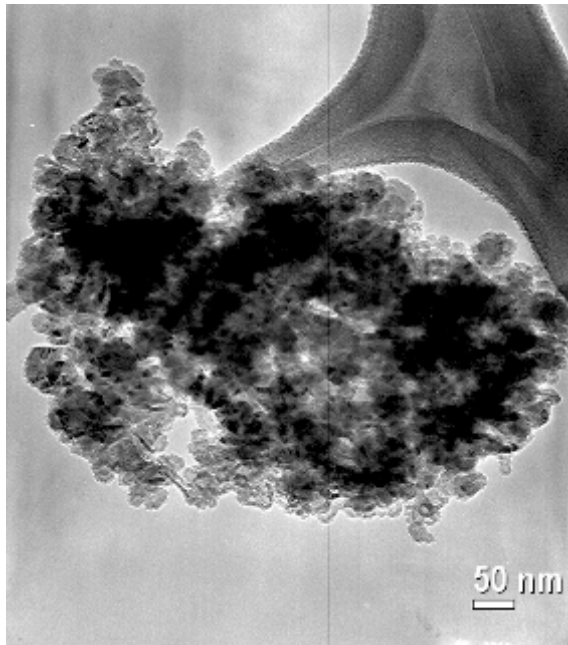
# Summary

- **From a comparison of particulate reactivity:**
  - ➔ **There is no definitive impact of initial nanostructure on oxidation rate**
  - ➔ **Under surface burning dominance during the early stage oxidation, the degree of internal structural change exerts a strong influence on the oxidation rate**
  - ➔ **The relative amount of initial oxygen groups is an important factor governing the soot oxidation rate**



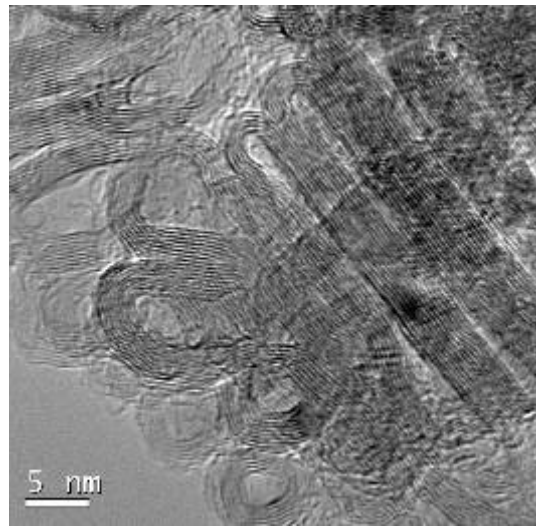
# B100 Soot

105k x

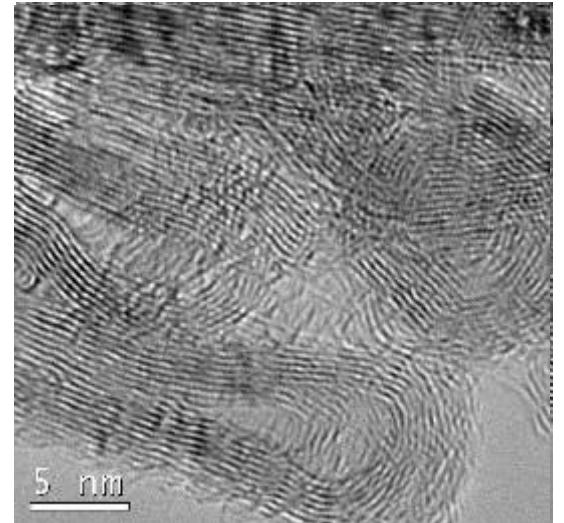
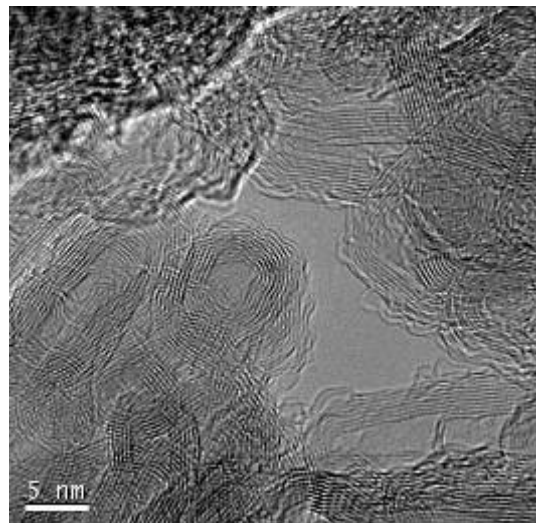
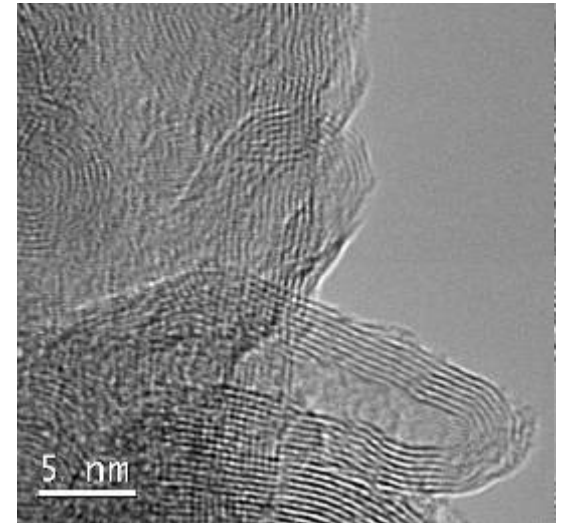


75% burn off, 50 min

500k x

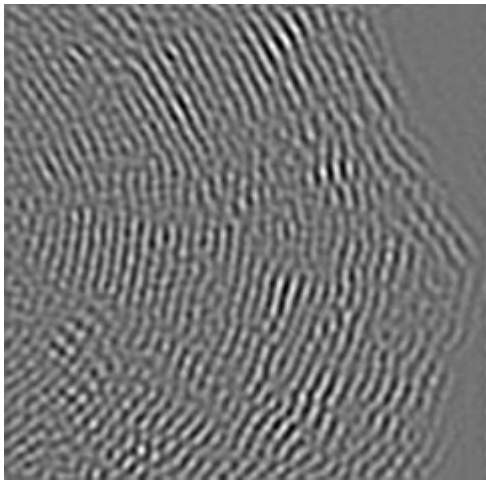


800k x

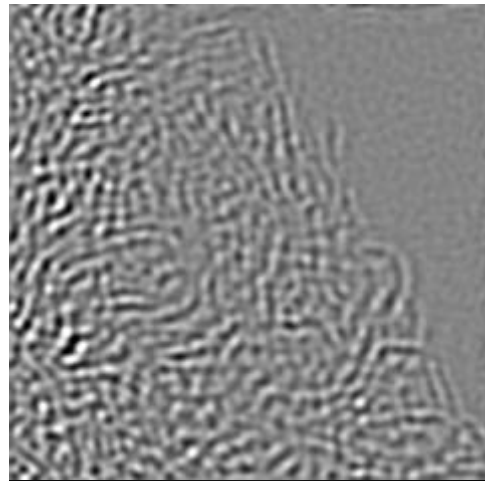


# Fringe Length Analysis - B100 Soot

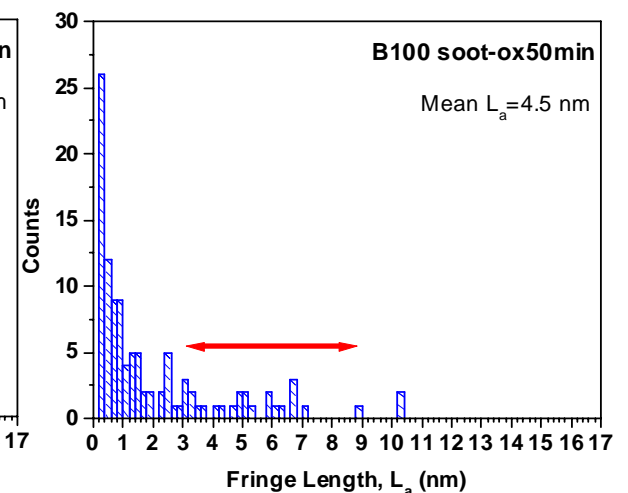
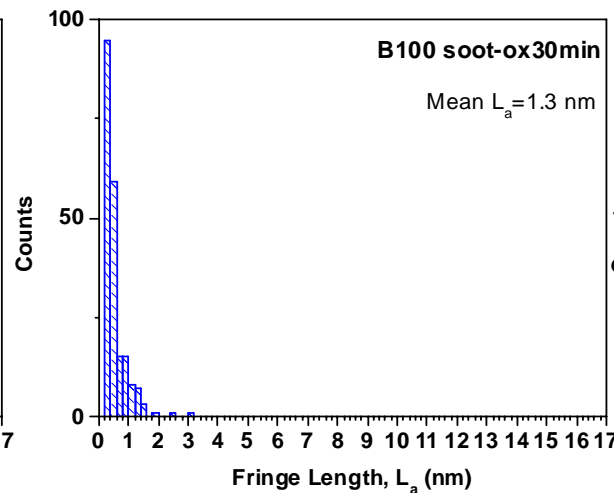
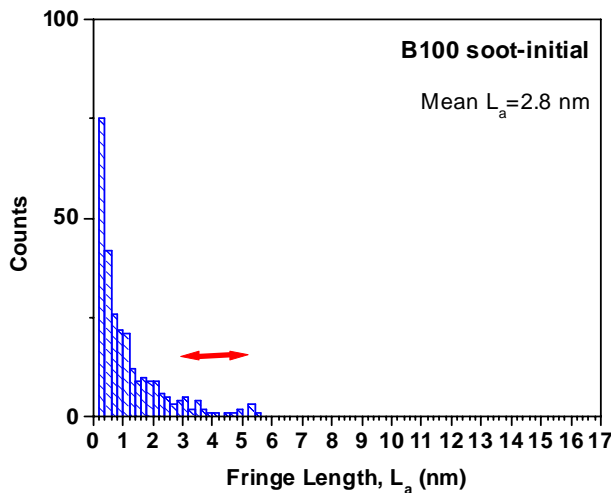
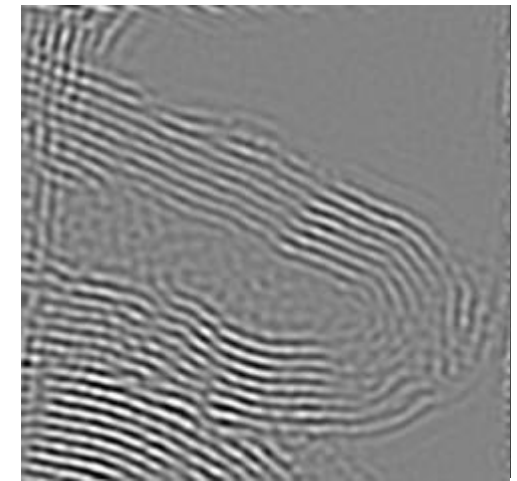
Initial



40% burnoff

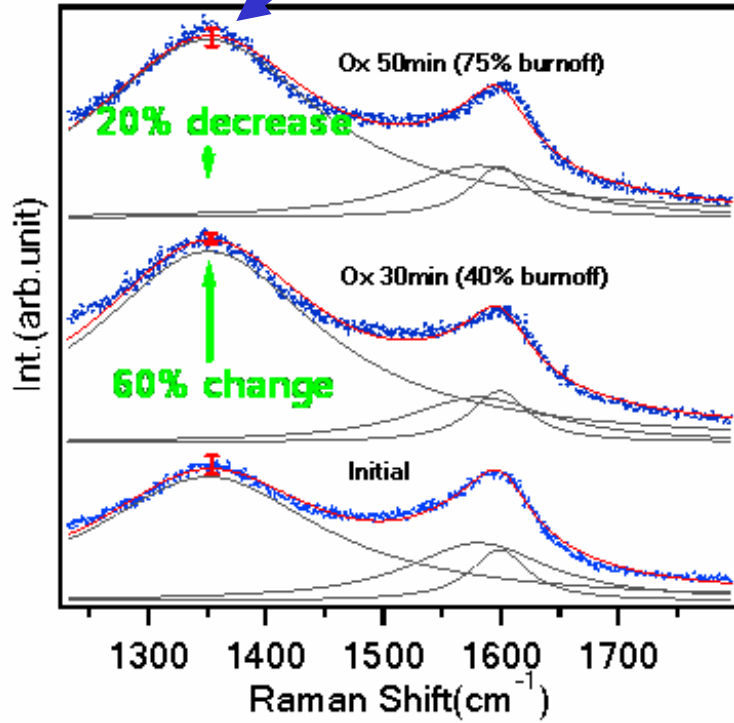


75% burnoff

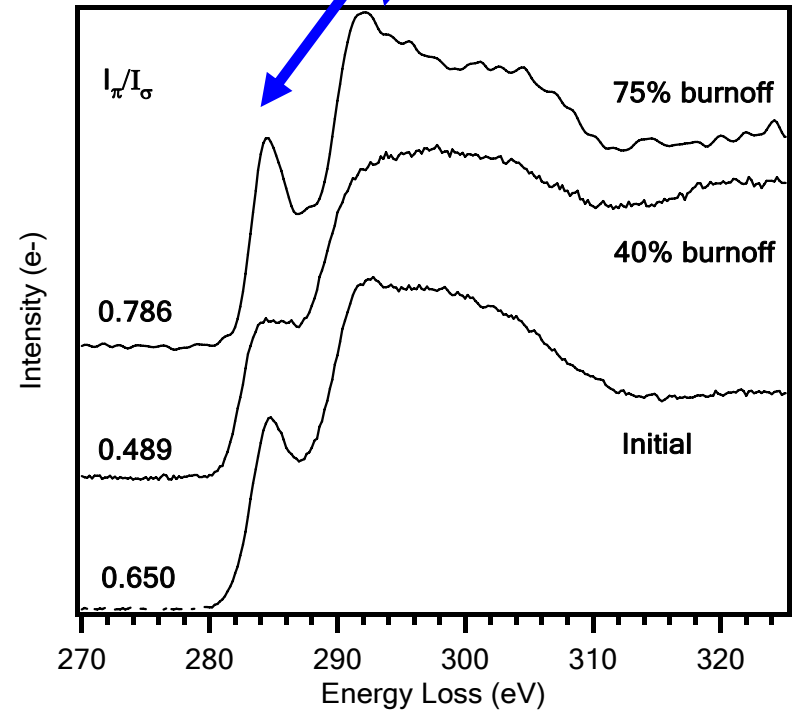




Decrease in D band

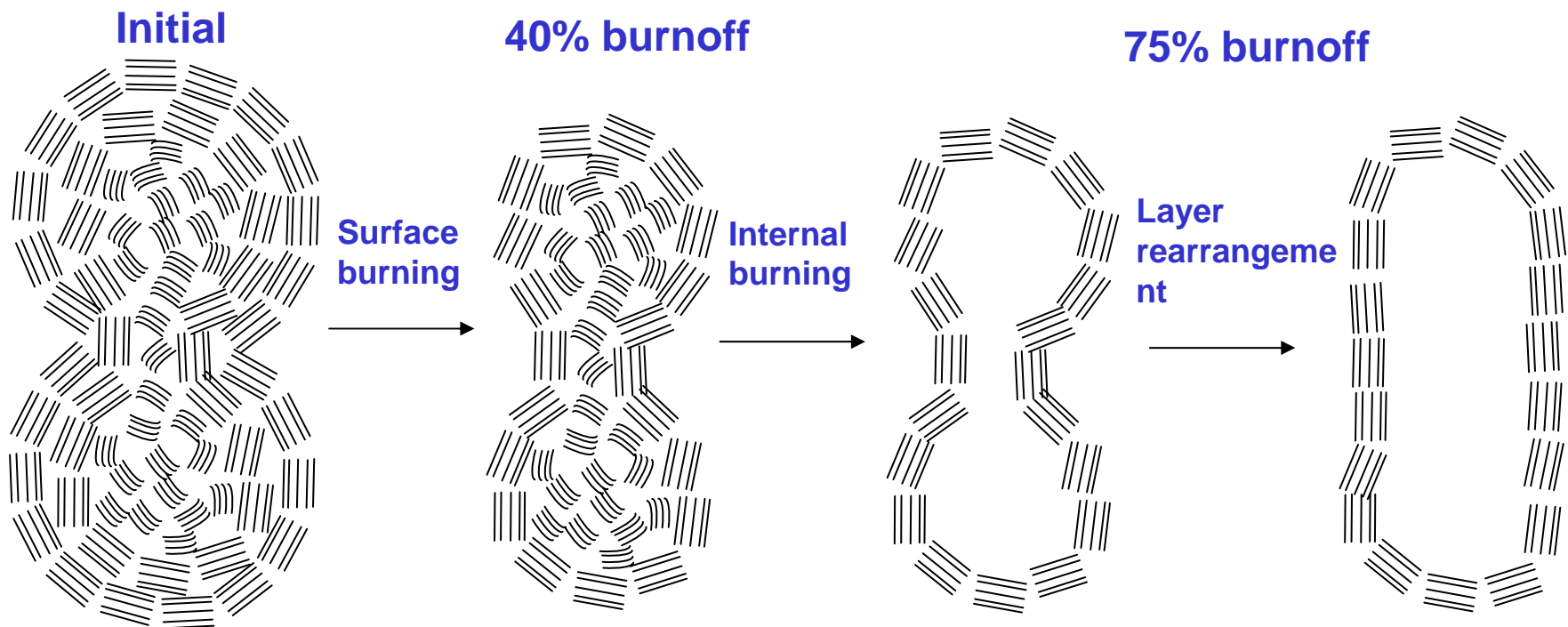


Prominent graphitic peak





# Oxidation Progression Model for B100 Soot



For simplicity, ignore crosslinking in this shell-core structure

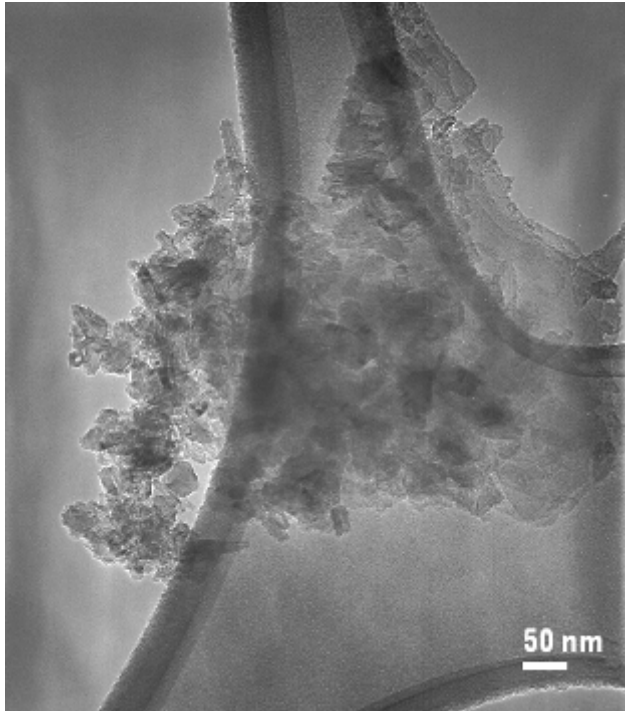
Once micro pore is fully penetrated, central hollow

Further coalescence, due to physical factor such as increase in layer mobility and minimizing a strain energy

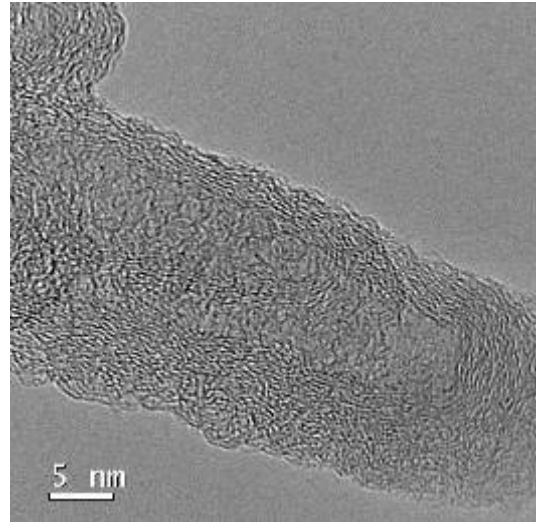


**FT Soot**

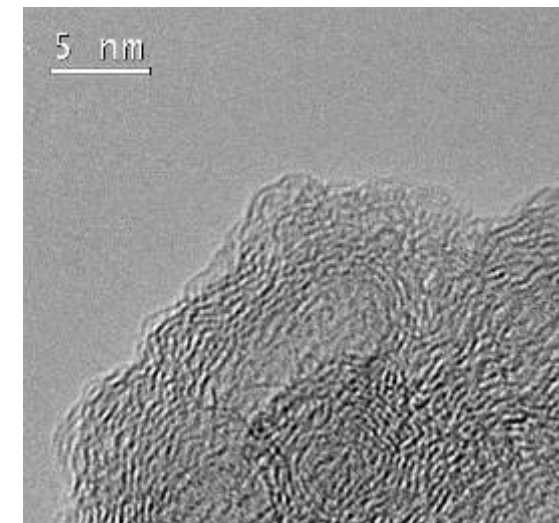
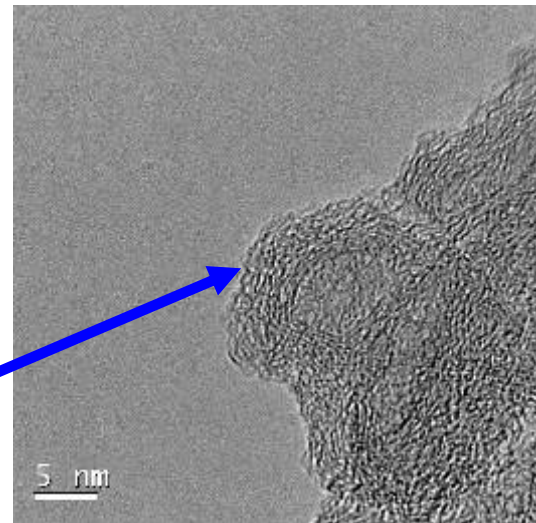
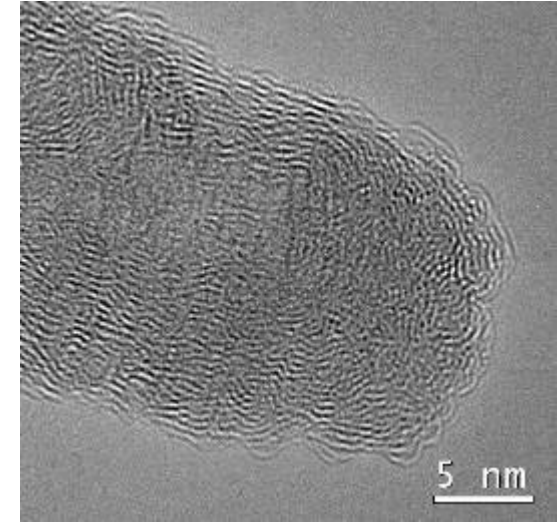
**105k x**



**500k x**



**800k x**



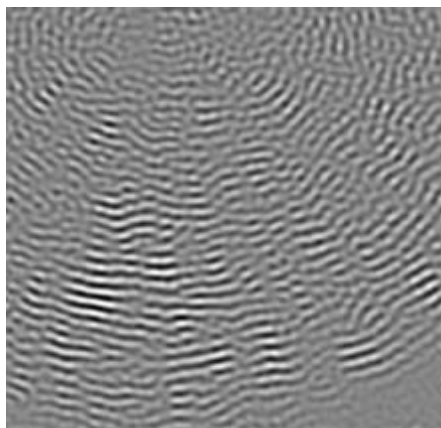
**75% burn off, 105 min**

**Still wavy and much shorter layer than B100**

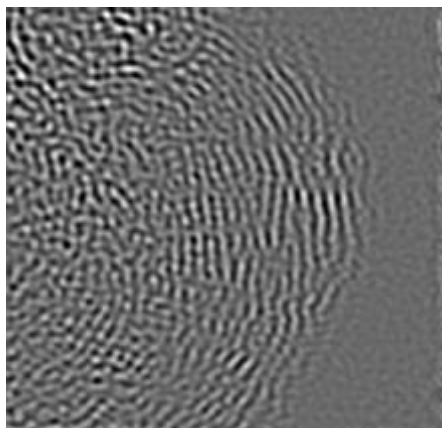


# Fringe Length Analysis - FT100 Soot

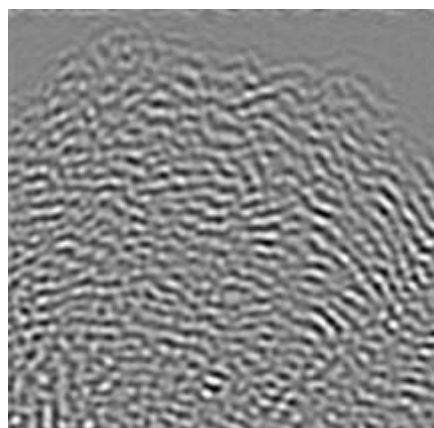
Initial



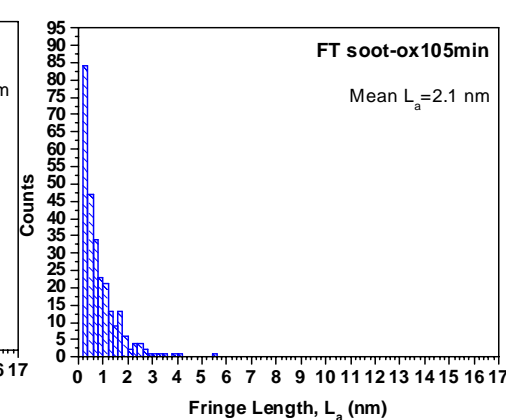
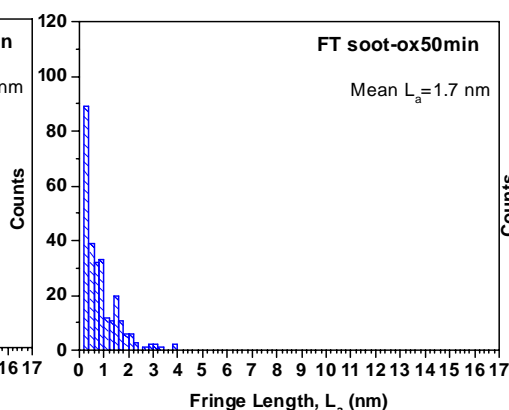
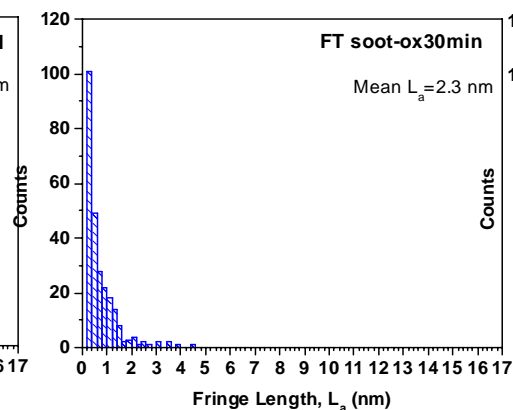
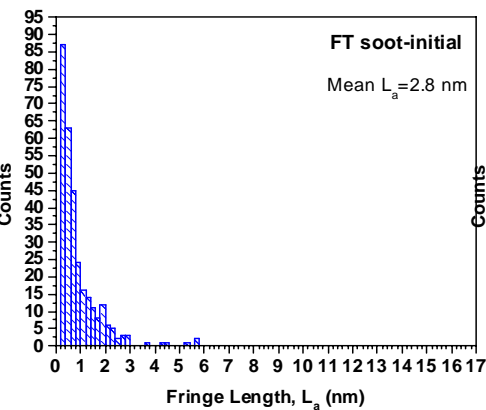
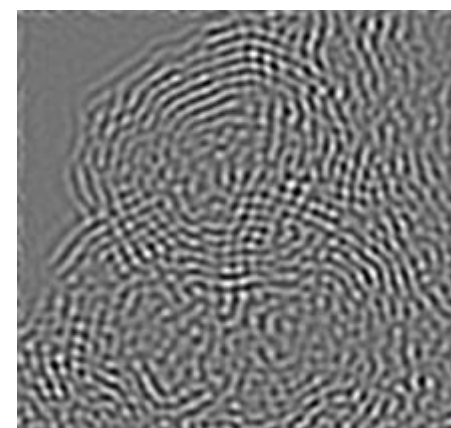
20% burnoff



40% burnoff

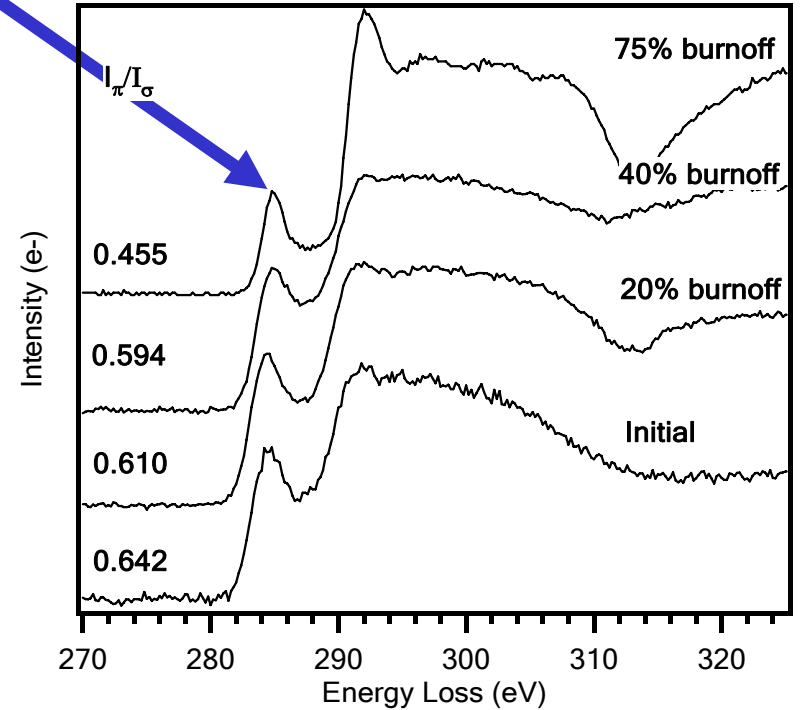
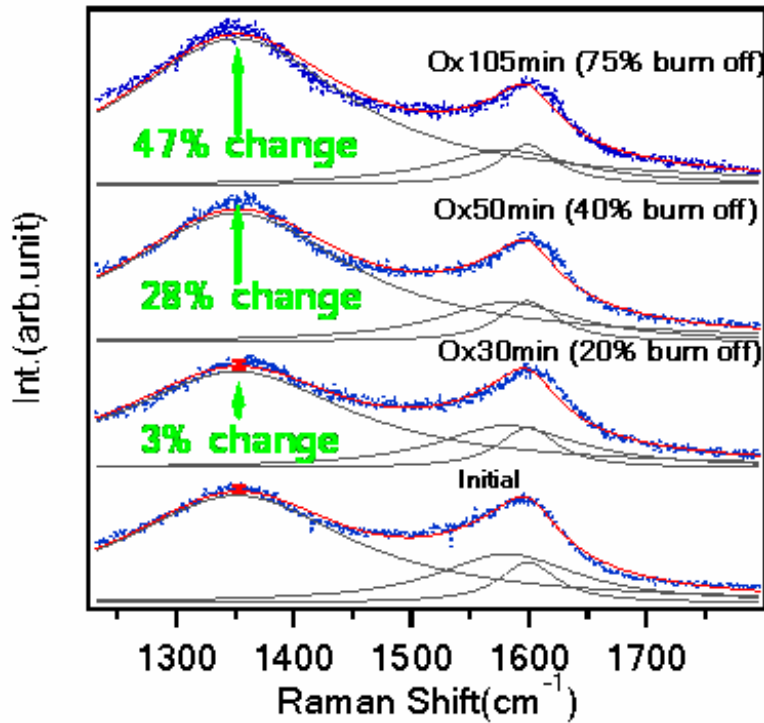


75% burnoff



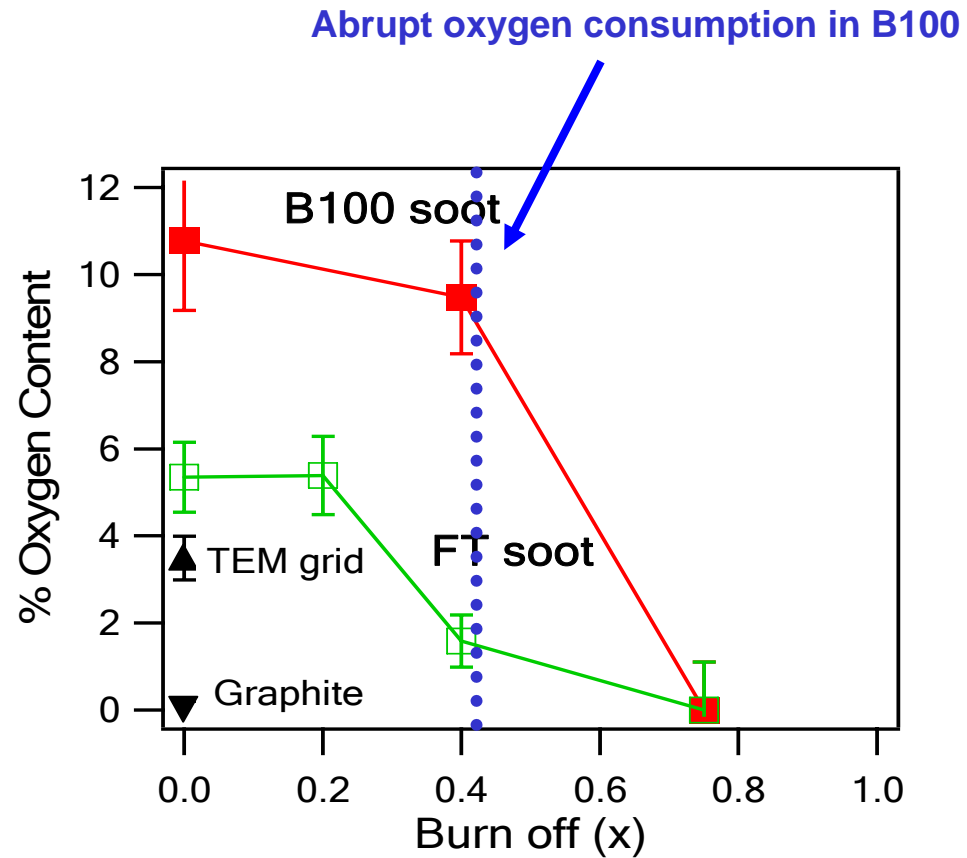
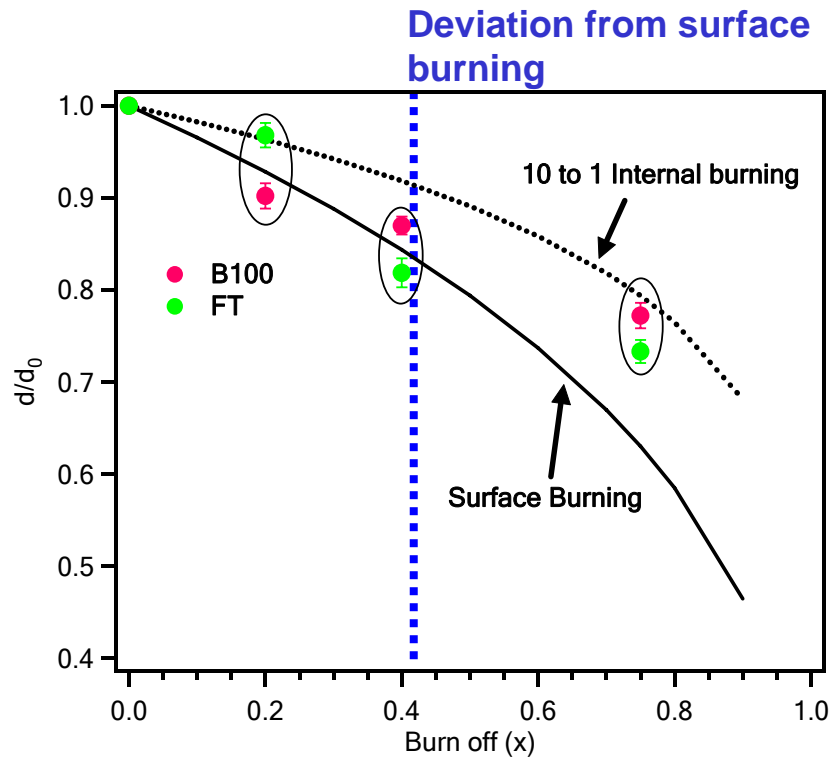


**Gradual increase in D band and decrease in relative ratio of graphitic peak suggesting a tendency toward disordered state**





# Comparison of Burning Regime





# Summary

- **B100 soot results in capsule type oxidation through internal burning, leading to a more ordered layer arrangement**
- **FT100 soot undergoes surface burning and less layer rearrangement than B100 soot, even at 75% burn off**
- **Early dramatic changes in inner structure and subsequent hollowing out of primary particles is a crucial factor in enhancing oxidation**
- **Surface reactivity involved in the early stage oxidation also seems to be responsible for a layer arrangement at later stage**



# Conclusions

- **Generalized Transition from surface burning to internal burning/layer rearrangement at later stage of oxidation**
- **Enhancement of oxidation and its unique process with B100 soot**
- **Importance of surface oxygen groups for a faster oxidation and layer arrangement**



# Acknowledgment and Disclaimers

- **Doug Smith, Kirk Miller, Etop Esen, Jim Rockwell, Rafael Espinoza, Keith Lawson and Ed Casey of ConocoPhillips**
- **US DOE-National Energy Technology Laboratory**
- **Edward Lyford-Pike, John Wright and Vinod Duggal of Cummins**
- **Ken Voss and Joe Patchett of Engelhard Corporation**
- **Howard Hess of Johnson-Matthey**
- **Dr. Farley Fisher of the National Science Foundation for supporting the acquisition of the AVL Videoscope (Grant# CTS-0079073)**
- **This presentation was prepared with partial support from the U.S. Department of Energy under Contract No. DE-FC26-01NT41098. The Government reserves for itself and others acting on its behalf a royalty-free, nonexclusive, irrevocable, worldwide license for Governmental purposes to publish, distribute, translate, duplicate, exhibit, and perform this copyrighted paper.**
- **This material was prepared with the support of the Pennsylvania Department of Environmental Protection. Any opinions, findings, conclusions, or recommendations expressed herein are those of the author(s) and do not necessarily reflect the views of the DEP.**